

**Princeton Plasma Physics Laboratory  
NSTX Experimental Proposal**

**Title: Influence of Hot Ions on Resistive Wall Mode Stability**

**OP-XP-932**

Revision: **2.1**

Effective Date: **5/12/09**  
*(Approval date unless otherwise stipulated)*  
Expiration Date:  
*(2 yrs. unless otherwise stipulated)*

**PROPOSAL APPROVALS**

**Responsible Author: J.W. Berkery**

Date 5/12/09

**ATI – ET Group Leader: S.A. Sabbagh**

Date 5/12/09

**RLM - Run Coordinator: R. Raman**

Date 5/12/09

**Responsible Division: Experimental Research Operations**

**Chit Review Board** (designated by Run Coordinator)

**MINOR MODIFICATIONS** (Approved by Experimental Research Operations)

# NSTX EXPERIMENTAL PROPOSAL

TITLE: **Influence of Hot Ions on Resistive Wall Mode Stability**

No. **OP-XP-932**

AUTHORS: **J.W. Berkery, S.A. Sabbagh, H. Reimerdes**

DATE: **5/12/2009**

## 1. Overview of planned experiment

The resistive wall mode (RWM) is thought to be stabilized by energy dissipation mechanisms that depend on plasma rotation and other parameters. Recently, a theory of kinetic resonances as passive RWM stabilization mechanisms has been explored<sup>1</sup>. The kinetic theory includes trapped and circulating thermal ions, trapped electrons, Alfvén resonances at the rational surfaces, and most recently, fast particles. Also, recently, JT-60U showed that energetic particle modes can act as triggers for resistive wall modes<sup>2</sup> (see Figure 1). The proposed experiment is to determine the influence of hot ions on the kinetic stability of resistive wall modes by varying the hot ion fraction. Experimental results will be compared to calculations from the MISK code. A similar experiment is also being run in DIII-D this year.

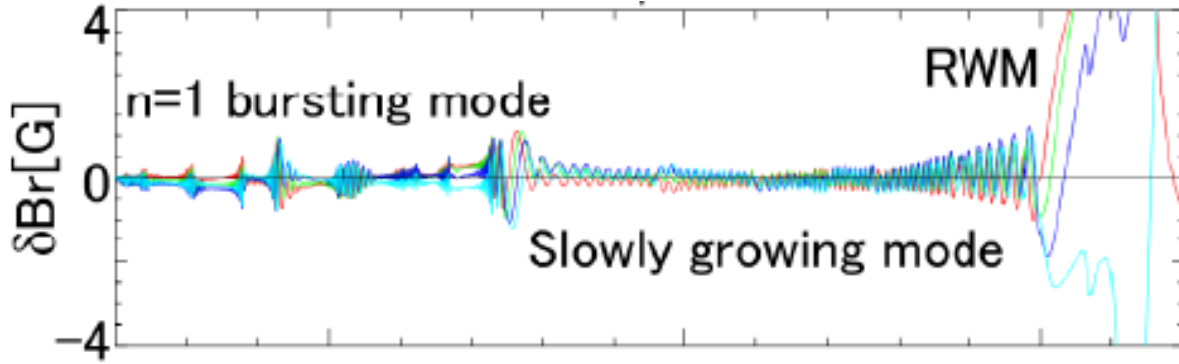


Figure 1: JT-60U results, showing an energetic particle mode triggering the resistive wall mode. (From Matsunaga, et al., IAEA 2009).

## 2. Theoretical/ empirical justification

The Modification to Ideal Stability by Kinetic effects (MISK) code calculates the contributions to the kinetic  $\delta W$ . In conjunction with PEST, which calculates the fluid and vacuum components, the RWM growth rate may be determined. The following equation shows the dependencies of the kinetic  $\delta W$  for thermal particles:

$$\delta W_K \propto \int_0^\infty \left[ \frac{\omega_{*N} + \left(\hat{\epsilon} - \frac{3}{2}\right) \omega_{*T} + \omega_E - \omega}{\langle \omega_D \rangle + l\omega_b - i\nu_{\text{eff}} + \omega_E - \omega} \right] \hat{\epsilon}^{5/2} e^{-\hat{\epsilon}} d\hat{\epsilon}$$

<sup>1</sup> B. Hu, R. Betti, and J. Manickam, *Phys. Plasmas* **12** (2005) 057301.

<sup>2</sup> G. Matsunaga et al., IAEA, 2009

where  $\nu_{\text{eff}}$  is the effective ion collisionality, and  $\omega_E$  is the  $E \times B$  frequency, which is directly related to the rotation frequency. We can immediately see that the plasma rotation enters the stability calculation in a somewhat complicated manner.

For energetic particles the calculation is different, since they have a different distribution. We use a slowing-down distribution function, and the result is the following dependence.

$$\delta W_K = \int_0^1 \frac{\epsilon_a \left( \frac{1}{\hat{\epsilon}^{\frac{3}{2}} + \hat{\epsilon}_c^{\frac{3}{2}}} \frac{d\hat{\epsilon}_c^{\frac{3}{2}}}{d\Psi} - \omega_f^a - \omega_{*N}^a \right) + \frac{3}{2} \frac{\hat{\epsilon}^{\frac{1}{2}}}{\hat{\epsilon}^{\frac{3}{2}} + \hat{\epsilon}_c^{\frac{3}{2}}} (\omega_E + \omega + i\gamma)}{\langle \omega_D \rangle + l\omega_b - i\nu_{\text{eff}} + \omega_E - \omega - i\gamma} \frac{\hat{\epsilon}^{\frac{5}{2}}}{\hat{\epsilon}^{\frac{3}{2}} + \hat{\epsilon}_c^{\frac{3}{2}}} d\hat{\epsilon}$$

Although this expression is somewhat more complicated, we can see that many of the same frequency resonances are present, such as the resonances with precession and bounce frequencies.

Figure 2 shows a stability diagram for NSTX shot 121083 @ 0.475s, just before the RWM was observed to experimentally go unstable. The solid line and markers are for the calculation without including hot ions. Values of the imaginary vs. the real components of  $\delta W_K$  are plotted for various levels of rotation, scaled from the experimental rotation profile. The value at “1.0” is quite close to the predicted marginal stability point (zero growth rate), in agreement with experimental observation. When hot ions are added to the calculation, the prediction is that the RWM is more stable over every rotation profile tested.

Although this prediction is farther from the experimental observation, it makes the important effect of hot ions clear. Theoretically, hot ions tend to add to the real part of the  $\delta W_K$ , increasing stability. Since the effect is significant, decreasing the hot ion fraction in experiments should lead to an observable change in the stability of the plasma.

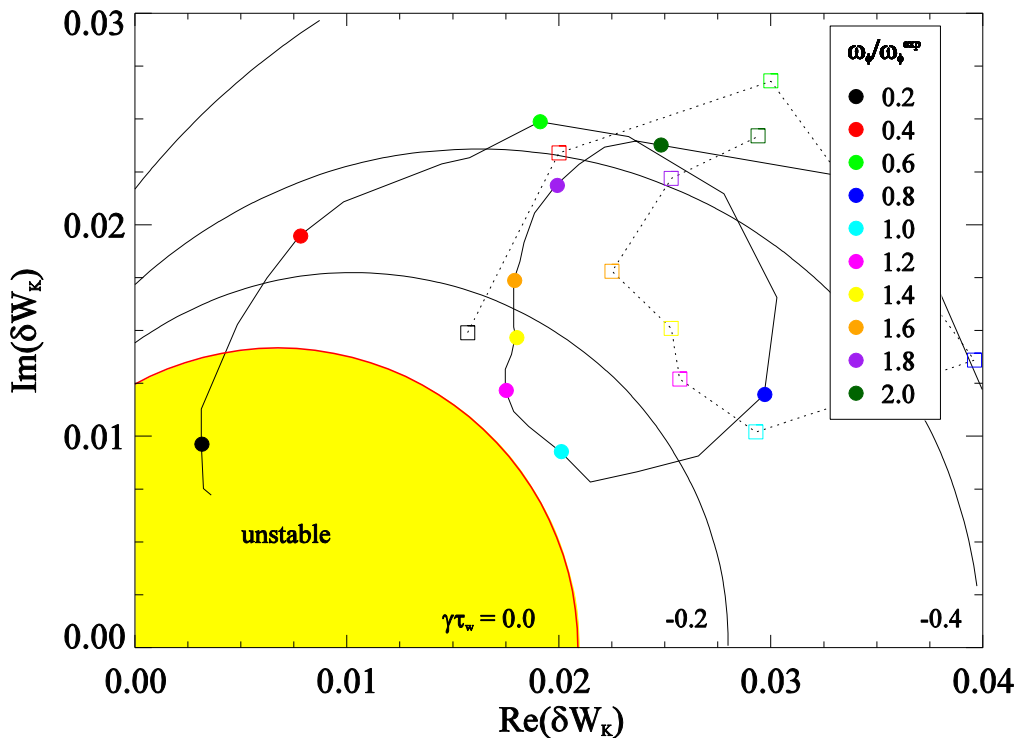


Figure 2: Stability diagram for NSTX shot 121083 @ 0.475s. The markers are for calculations with the plasma rotation profile scaled as indicated. The solid line and markers are without hot ions, while the dashed line and open markers are with hot ions.

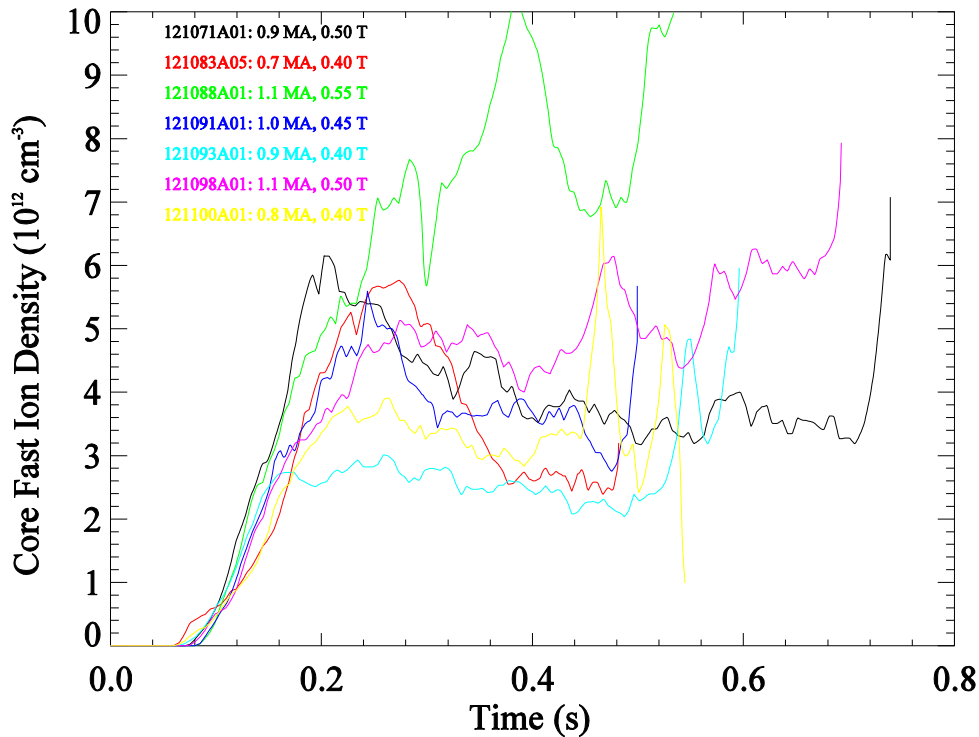


Figure 3: Core fast ion density vs. time for multiple shots with varying plasma current and magnetic field, as calculated by TRANSP.

There are three main methods we can use to control the hot ion fraction. First, the hot ion density has been seen to correlate with the toroidal magnetic field. Figure 3 shows the core hot ion density, calculated by TRANSP, vs. time for seven shots from XP619 (Sontag, 2006). These shots span a variety of plasma currents and toroidal fields. A correlation between field and hot ion density can be seen, with the difference between the minimum and maximum being about a factor of three. Changing the field (at constant  $q$ ) will be the main control over hot ion fraction in this experiment.

The second method of controlling the fast ion density is through the beam voltages. In XP840 (Stutman, 2008), beam source B was changed between two shots from 80kV to 70kV (which does change the neutral beam injected power slightly). TRANSP analysis shows that this change resulted in a  $\sim 20\%$  reduction in fast particle density (Fig. 4, after 0.45s). In the same XP there was also a pair of shots in which the same total beam power was maintained, while the beam voltages were changed from 95kV on B to 65kV each on B and C (Fig. 5). In this case, the core fast particle density also dropped about 20%. The third way to control hot ion fraction is through the slowing down time. The fast ion slowing down time is inversely dependent on the plasma density. By increasing the density, the slowing down time is decreased and therefore the hot ion fraction is decreased. This control will be principally employed in a similar experiment this year on DIII-D. In NSTX we can employ lithium to change the plasma density profile. So far, TRANSP analysis does not show a large effect of lithium on the hot ion profile.

Similarly, the FIDA diagnostic failed to see a large effect of lithium on fast ion profiles from shots this year<sup>3</sup>. Also, XP905 (Darrow, 2009) recently attempted to change the plasma density from shot to shot by changing the gas injection, but was unsuccessful. This strategy will therefore be reserved as an additional possible method of control over the hot ion fraction in this experiment, if further run time is allocated and more analysis, or shot development, is performed that shows the promise of this method.

<sup>3</sup> Personal communication with Mario Podesta.

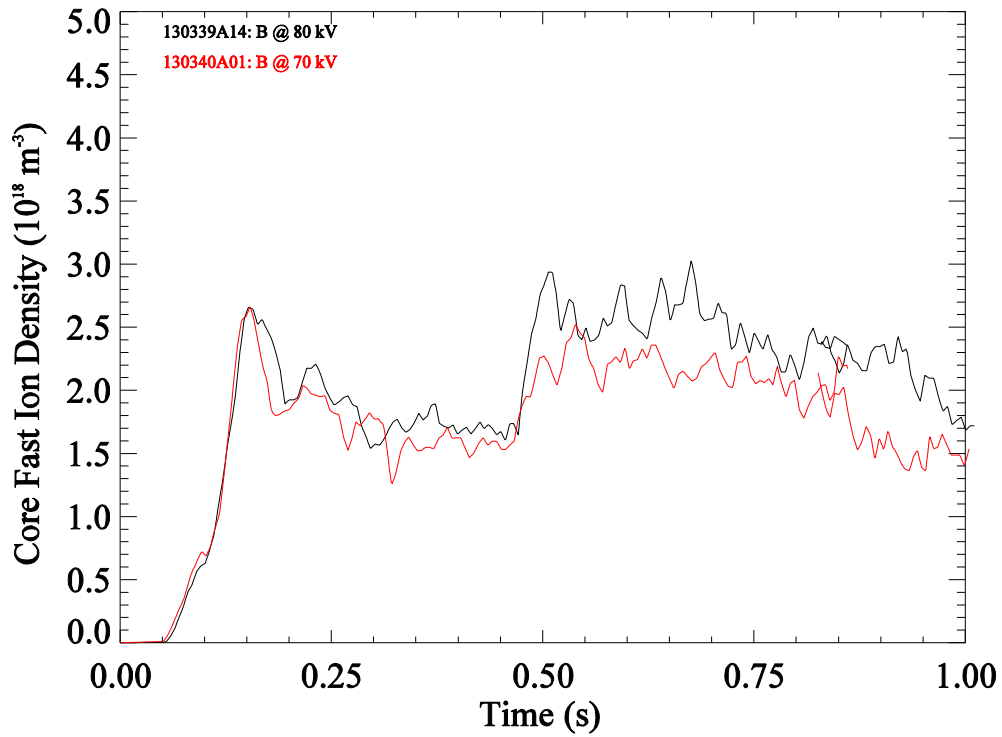


Figure 4: Core fast ion density vs. time for two shots from XP840, which have different source B beam voltages starting at 0.45s, as calculated by TRANSP.

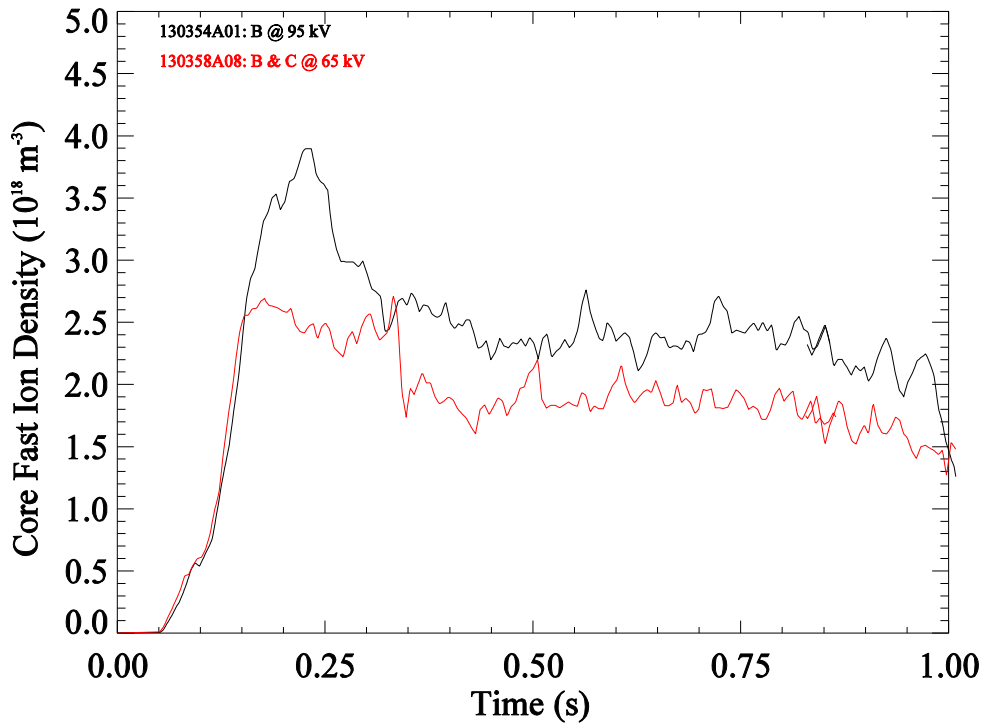


Figure 5: Core fast ion density vs. time for two shots from XP840, which have different beam voltages at the same total beam power, as calculated by TRANSP.

### 3. Experimental run plan

Task Number of Shots

- 1) Establish target
  - A) Start lithium deposition
  - B) Use 130232 as setup shot (relatively high elongation  $\sim 2.3$  to avoid rotating modes,  $I_p = 0.9$  MA,  $B_t = 0.45$ T), start  $n=3$  correcting field at 0.250 s, ramping to full amplitude at 0.300 s. Use 90kV on sources A, B, and C, and change timing on C if necessary. 3
  
- 2) Vary the  $n=3$  DC field timing and magnitude
  - A) Correct  $n=1$  error field using feedback system,  $B_p$  sensor filter time = 100 ms. 3
  - B) During the period devoid of  $n=1$  rotating mode activity, vary the  $n=3$  DC field from correcting phase to braking phase, and vary the SPA current ramp rate and timing to optimally change plasma rotation, to find the marginal point. 6
  
- 3) Vary the plasma current and toroidal field to change the fast particle density  
 Repeat the above procedure for the next two conditions, still with lithium.

Condition	$I_p$ (MA)	$B_t$ (T)	Shots
1	0.9	0.45	(already done above)
2	0.7	0.35	6
3	1.1	0.55	6

If the conditions can be completed quickly, we could add two more:  $I_p = 0.8$  MA,  $B_t = 0.40$ T, and  $I_p = 1.0$  MA,  $B_t = 0.50$ T, or we could move on to step four.

- 4) Vary the neutral beam voltage for one of the above conditions
  - A) Choose the above current/field condition that is working best and change the beam voltages at constant power. First, using either source B or C only changes the deposition profile. Then reducing the voltage on both B and C changes the fast ion density. 3
  - B) Reduce source C from 90kV to 80kV, 70kV and 60kV (This will change the total beam power). 3

Beam A (kV)	Beam B (kV)	Beam C (kV)	Beam Power (MW)	Shots
90	95	0	4	1
90	0	95	4	1
90	65	65	4	1
90	90	90	6	(already done above)
90	90	80	?	1
90	90	70	?	1
90	90	60	?	1

Total: 30

#### 4. Required machine, NBI, RF, CHI and diagnostic capabilities

See attached Physics Operations Request and Diagnostic Checklist.

The FIDA diagnostic will be used to monitor the fast ion population for each shot. Unfortunately, FIDA requires a low plasma density ( $<5 \times 10^{19} \text{ m}^{-3}$ ) in order to achieve good signal to noise. This means that we will probably only be able to get measurements with low error bars for the edge fast ion population. However, we will use this information to determine whether we are making a difference in hot ion fraction from shot to shot. Mario Podesta has provided a comparison of the shots shown in Fig. 5. The results, shown in Fig. 6, although in arbitrary units, show a large effect of beam voltage on the fast ion distribution.

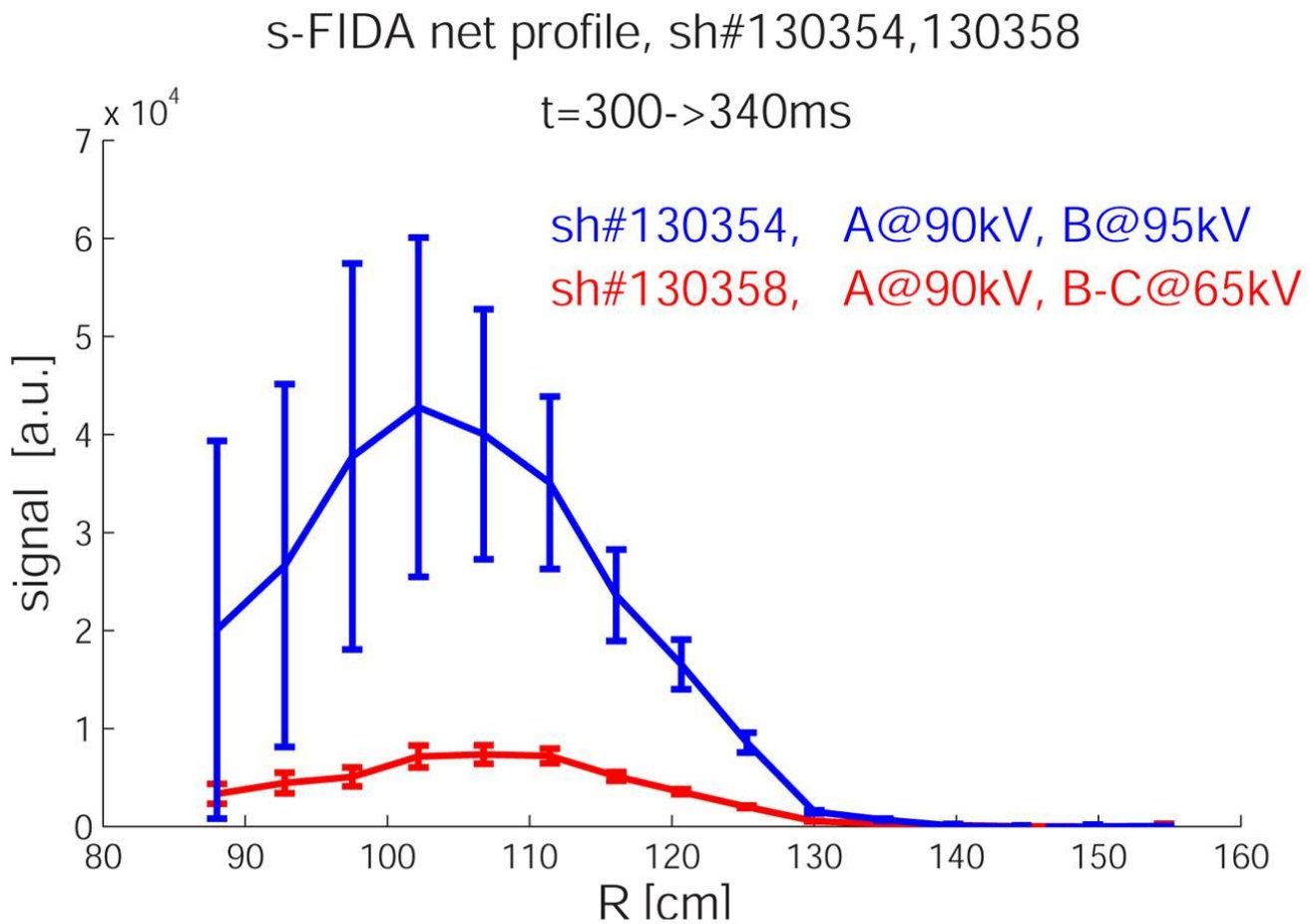


Figure 6: FIDA analysis for two shots from XP840, which have different beam voltages at the same total beam power.

## **5. Planned analysis**

Equilibrium reconstructions will be performed with EFIT, with MSE and the flux iso-surface constraint, for reduced error on the  $q$  profile. These equilibria will then be analyzed with PEST to obtain the fluid stabilization and MISK to obtain the kinetic stabilization.

## **6. Planned publication of results**

This experiment is a critical step towards reaching the FY09 milestone on understanding RWM stabilization physics as a function of plasma rotation, and delves into the role of fast ions for the first time. If results and subsequent comparison to theory yields a significant new understanding of RWM kinetic stabilization, the results will be suitable for publication in Physical Review Letters. Results that are not at the level of novelty for a PRL publication will be sent to Physics of Plasmas. Any clear conclusions from this experiment are expected to be presented at the APS conference in Atlanta, November 2009.

# PHYSICS OPERATIONS REQUEST

TITLE: **Influence of Hot Ions on Resistive Wall Mode Stability** No. **OP-XP-932**

AUTHORS: **J.W. Berkery, S.A. Sabbagh, H. Reimerdes** DATE: **5/12/2009**

**Describe briefly the most important plasma conditions required for the XP:**

High beta plasma with a long MHD free phase. Will be changing plasma current and field, RWM coils currents and timing, and beam voltages.

**List any pre-existing shots: 132723 ( $I_p = 1.1$  MA,  $B_t = -0.55$  T)**

**Equilibrium Control:** Gap Control / rtEFIT(isoflux control):

Machine conditions (*specify ranges as appropriate, use more than one sheet if necessary*)

$I_{TF}$  (kA): **0.3 – 0.55 T** Flattop start/stop (s):

$I_p$  (MA): **0.6 – 1.1 MA** Flattop start/stop (s):

Configuration: **Limiter / DN / LSN / USN** (*strike out inapplicable cases*)

Outer gap (m): **0.06 – 0.10** Inner gap (m): **0.04** Z position (m):

Elongation  $\kappa$ : **2.1 – 2.5** Upper/lower triangularity  $\delta$ : **0.45 – 0.75**

Gas Species: **D** Injector(s):

NBI Species: **D** Voltages (kV or off) **A: 90 B: 60-100 C: 60-100** Duration (s):

ICRF Power (MW): Phasing: Duration (s):

CHI: **Off / On** Bank capacitance (mF):

LITERs: **Off / On** Total deposition rate (mg/min): **15**

EFC coils: **Off/On** Configuration: **Odd / Even / Other** (*attach detailed sheet*)

## DIAGNOSTIC CHECKLIST

**TITLE: Influence of Hot Ions on Resistive Wall Mode Stability**

**No. OP-XP-932**

**AUTHORS: J.W. Berkery, S.A. Sabbagh, H. Reimerdes**

**DATE:**

*Note special diagnostic requirements in Sec. 4*

Diagnostic	Need	Want
Bolometer – tangential array		√
Bolometer – divertor		√
CHERS – toroidal	√	
CHERS – poloidal		√
Divertor fast camera		√
Dust detector		√
EBW radiometers		√
Edge deposition monitors		√
Edge neutral density diag.		√
Edge pressure gauges		√
Edge rotation diagnostic		√
Fast ion D <sub>α</sub> - FIDA	√	
Fast lost ion probes - IFLIP		√
Fast lost ion probes - SFLIP		√
Filterscopes		√
FIReTIP		√
Gas puff imaging		√
H $\alpha$ camera - 1D		√
High-k scattering		√
Infrared cameras		√
Interferometer - 1 mm		√
Langmuir probes – divertor		√
Langmuir probes – BEaP		
Langmuir probes – RF ant.		
Magnetics – Diamagnetism	√	
Magnetics – Flux loops	√	
Magnetics – Locked modes	√	
Magnetics – Pickup coils	√	
Magnetics – Rogowski coils	√	
Magnetics – Halo currents		√
Magnetics – RWM sensors	√	
Mirnov coils – high f.		√
Mirnov coils – poloidal array	√	
Mirnov coils – toroidal array	√	
Mirnov coils – 3-axis proto.		

*Note special diagnostic requirements in Sec. 4*

Diagnostic	Need	Want
MSE	√	
NPA – ExB scanning		√
NPA – solid state		√
Neutron measurements	√	
Plasma TV		√
Reciprocating probe		
Reflectometer – 65GHz		√
Reflectometer – correlation		√
Reflectometer – FM/CW		√
Reflectometer – fixed f		√
Reflectometer – SOL		√
RF edge probes		
Spectrometer – SPRED		√
Spectrometer – VIPS		√
SWIFT – 2D flow		
Thomson scattering	√	
Ultrasoft X-ray arrays	√	
Ultrasoft X-rays – bicolor		√
Ultrasoft X-rays – TG spectr.		√
Visible bremsstrahlung det.		√
X-ray crystal spectrom. - H		√
X-ray crystal spectrom. - V		√
X-ray fast pinhole camera		√
X-ray spectrometer - XEUS		√